International Journal of Robotics and Control Systems
Vol. 4, No. 3, 2024, pp. 1075-1091
ISSN 2775-2658
http://pubs2.ascee.org/index.php/ijrcs

Applications of Multi-Objective OPF Solutions with Optimal Placement of Multiple and Multi-Type FACTS Units to IEEE System: Comparison of Different Approaches

Sultan Hassan Hakmi [a,1,*]

[a] Department of Electrical and Electronic Engineering, College of Engineering and Computer Science Jazan University, Jazan 45142, Saudi Arabia
[1] shhakmi@jazanu.edu.sa
* Corresponding Author

ARTICLE INFO

Article history
Received May 08, 2024
Revised June 23, 2024
Accepted July 01, 2024

Keywords
Multi-Objective Optimization;
Power System Stability;
FACTS;
IEEE 30 Bus;
Multiple GUPFCs

ABSTRACT

Optimal power flow (OPF) problem and its implications for power system stability and efficiency is investigated in this study. OPF, a restricted optimization query with non-linearity and non-convexity, is one of the most challenging and fascinating problems in the recent power system. Based on these parameters, researchers have been working hard over the past few decades to identify the best solutions to the OPF issue that maintain system stability. This work presents multi-objective OPF solutions utilizing Newton's technique with numerous multi-type FACTS units. First, the GA is applied to identify the perfect size and location of the FACTS units. Next, the generator and FACTS settings are optimized. In this instance, four scenarios are taken into consideration and three OFs are employed to see how the OFs affect the positioning and dimensions of FACTS devices. The OF is suggested to consider the reduction of both generation costs and transmission losses while also optimizing the power transfer capacity of designated corridors. A full analysis relating to the IEEE-30 bus system is presented and analyzed.

1. Introduction

The worrisome rise in demand's and dynamic's load trends, which have a substantial impact on TSs, have made electrical grids into ever more complicated systems. They frequently operate as over\underloaded [1]-[5]. Most nations still use antiquated TSs. For instance, the 345 kV bulk TSs in the US and their related substations, cables, and wires are forty years of age or older [6]. Furthermore, the costly nature of building and developing novel ESs means that several difficult problems already in place, like excessive power losses, voltage profile concerns, instability as well as reliability challenges, will inevitably get worse [1], [7]-[9]. The homes, businesses, and manufacturing industries are predicted to grow by 0.5%, 0.8%, and 0.9% yearly from 2013 to 2040, based on research by the EIA [10]-[12]. Nevertheless, is not anticipated that the system will be able to satisfy the need and send the electricity produced from centralized PG to the distribution system by 2040, according to the same report [10], [13]-[15]. Approximately 1134.6 GW of PG capacity would be needed. The TS may get congested as a result of this [16]-[18]. Making the maximum use of the PG and TSs is therefore the wisest course of action.

The most important method for minimizing generation costs and TS losses while also maximizing power move ability trends in an ES with current transmission and operating limitations is known as OPF. OPF solution strategies are crucial for controlling PFs in a market that has been privatized. Several optimization methods have been used for OPF problems throughout the past 40 years [19]-[21]. They can be categorized as Newton-based approaches, EP approaches, interior methods (IM), GA, etc. Nonlinear objective and constraint equations are used in nonlinear programming techniques. Because they can simulate ESs quite well, these constitute the oldest class of OPF approaches. A strategy to reduce fuel expenses and active power (P) loss through the use of the penalty function optimization methodology is covered in [22]. Ref [23] optimizes shifted cost models using a modified version of Fletcher's quasi-NM. Problems involving constraints and goal functions expressed in linear forms are handled by LP. Ref [24] used an LP technique to solve an financial dispatch of P with constraint lessening. Ref [25] divided the dispatch challenge into a dominant difficulty and multiple smaller LP subdivisions via the Dantzig-Wolfe breakdown. The NM in conjunction with linear programming techniques has been covered in [26]. Refs. [27], [28], uses an optimizing technique that involves splitting the initial problem into a set of linearly bound subdivisions and solving them with an enriched Lagrangian-style objective function.

To give ESs the most benefits, diverse types of FACTS devices, like the UPFC, TCSC, SSSC, SVC, STATCOM, TCPST, TCVR, interlink PF controller, and optimal UPFC, should have their types, numbers, positions, and settings optimized [29]-[32]. The best places and contableurations for FACTS units in ESs are difficult to determine, and a sizable data collection is usually needed. Four types of approaches and techniques were employed in earlier studies to identify the best locations and configurations for FACTS tools: analytical techniques, mathematical coding approaches, meta-heuristic optimization ways, and hybrid techniques. The capacity of FACTS regulators to adopt algorithms of control constructed to accomplish numerous goals is one of its distinguishing features [33]-[35]. The optimal place of FACTS units is a multi-objective optimization problem, including the power balance equation, bus voltage, producer P&Q, ratings for FACTS tools, TS thermal bounds, power loss formula, PF equations, and request restrictions [36], [37].

The exceptionally nonlinear OPF issue can be solved using GA, which was suggested in [38], [4] and is not limited by the fuel cost functions' shape. To carry out its genetic processes, GA needs an encoding method for deciding parameters, though. The convergence of the GA is significantly impacted by various encoding techniques. Extensive computer time is also wasted on the crossover and mutation operations on binary-coded parameters, as well as the encoding and decoding for each option that is found. The efficacy of the GA in resolving the OPF issue is diminished by these issues. The optimization problem for units with non-smooth fuel cost has been addressed in recent papers using EP approaches that can incorporate all limitations resulting from FACTS units and liberalization. NM was used in [39] to solve the OPF including advanced SVC and UPFC. Ref. [40] used nonlinear IM to solve OPF including GUPFC. The best places for FACTS tools in vertically integrated and unbundled ESs can be found using a variety of indices and methodologies [38]. To minimize mathematical complexity, GA approaches can be applied to determine the best position for FACTS tools for various goal functions [41], [42].

Regardless of system size, the suggested OPF algorithm can handle multiple TCSC, UPFC, and GUPFC units in addition to multi-type FACTS. The approach makes use of patchy NM, which allows for a noteworthy lessening in both the mathematical involvedness and the solution time without sacrificing optimality. Many variables are analyzed, such as the voltage magnitude and phase angle, PG cost, setting up and operating costs of FACTS tools (place, sort, amount, and bulk), and overloaded and utilization lines. The IEEE 30 bus system standard is castoff to prove the role of the wished-for systems.

2. Problem Formulation

2.1. OPF with FACTS Devices

The next form can be used to define a broad minimizing issue: Maximize/Minimize $f(x,u,s)$ (OF) Subject to:

$$g(x,u,s) = 0 \text{ (EC)}$$
$$\text{and } h(x,u,s) \leq 0 \text{(IC)} \tag{1}$$

where vectors x, u, and s are state, control, and FACTS variables and fully described in [43], [44]:

$$x = [Q_{G1}, \cdots Q_{Gn}, \delta_{G1}, \cdots \delta_{Gn}, V_{PQ1}, \cdots V_{PQn}, \delta_{PQ1}, \cdots \delta_{PQn}]^T \tag{2}$$

$$u = [P_{G1}, \cdots P_{Gn}, V_{G1}, \cdots V_{Gn}, Tap_1, \cdots Tap_{nT}]^T \tag{3}$$

$$s = [s_{TCSC}, s_{UPFC}, s_{GUPFC}, \cdots]^T \tag{4}$$

where $s_{TCSC} = X_{TCSC}$, is the reactance of the TCSC, $s_{UPFC} = [\delta_{sUPFC}, V_{sUPFC}, \delta_{pUPFC}]^T$ are the VM and angle of series and shunt inserted voltage of the UPFC and $s_{GUPFC} = [\delta_{slGUPFC}, V_{slGUPFC}, \delta_{pGUPFC}]^T$ are the VM and angle of series and shunt inserted voltage of GUPFC. All the variables of x, u and **s** are the decision variables of the $f(x,u,s)$. It plots the VS ($n_u + n_x + n_s$) onto scalar space. $g(x,u,s)$ is the function in lieu of the ECs. Its atlases the ($n_u + n_x + n_s$) VS onto a VS of size *k*. ECs are the PF equations. $h(x,u,s)$ is the function representing the ICs. It maps the ($n_u + n_x + n_s$) VS onto a VS of size *m*. ICs are the PFs and voltage profiles, besides TSs flows.

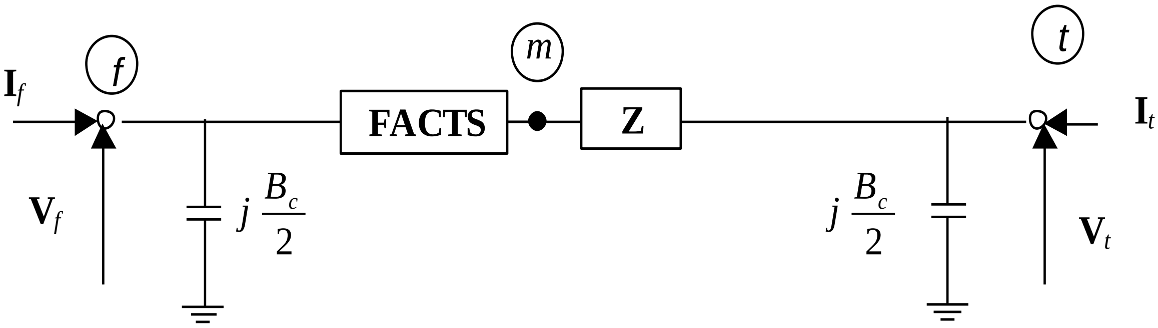

Fig. 1. TS including FACTS

For simplification, all the variables in x and u can be combined to x and so we can assume an OF with EC and IC are the function of x, s only.

The EC's OF $g(x,s)$ and IC $h(x,u,s)$is given as seen in (5), and (6)

$$g(x,s) = [g_{p_1}(x,s), \dots g_{p_n}(x,s), g_{Q_1}(x,s), \dots g_{Q_n}(x,s)]^T = \begin{bmatrix} \Delta P \\ \Delta Q \end{bmatrix} = 0 \tag{5}$$

$$h(x,u,s) = \left\{ \begin{bmatrix} h_1(x,u) \\ h_2(s) \end{bmatrix} \right\} \leq 0 \tag{6}$$

Where (7), As seen in (8), the optimization process terminates as soon as the variations amid the defined and determined apparent line powers are smaller than a preset lenience.

2.2. Lagrangian Function (LF)

Through NM, the system's nodal VMs, angles, and FACTS state variables are integrated into a single frame as a basis to provide a unified, ideal solution. The given PF, VMs, and optimality requirements are satisfied automatically by regulating the FACTS state variable [45]. Based on the equivalent circuit (Fig. 1).

$$h_1(\boldsymbol{x},\boldsymbol{u})\left\{=\left[\begin{array}{l} {P_{Gi}}^{min_{Gi}} \\ P_{Gi}-{P_{Gi}}^{max} \\ {V_{Gi}}^{min_{Gi}} \\ V_{Gi}-{V_{Gi}}^{max} \\ {T_i}^{min_i} \\ T_i-{T_i}^{max} \\ {Q_{Gi}}^{min_{Gi}} \\ Q_{Gi}-{Q_{Gi}}^{max} \\ {V_i}^{min_i} \\ V_i\ -{V_i}^{max} \\ \left[S_{ft}\right]^2-\left[{S_{ft}}^{max}[]^2\right][]\{\}\leq 0, h_2(\boldsymbol{s})=\left[\begin{array}{c} X_{TCSC}^{min_{TCSC}} \\ X_{TCSC}-X_{TCSC}^{max} \\ V_{sUPFC}^{min_{sUPFC}} \\ V_{sUPFC}-V_{sUPFC}^{max} \\ \delta_{sUPFC}^{min_{sUPFC}} \\ \delta_{sUPFC}-\delta_{sUPFC}^{max} \\ \delta_{pUPFC}^{min_{pUPFC}} \qquad \leq 0 \\ \delta_{pUPFC}-\delta_{pUPFC}^{max} \end{array}\right] \end{array}\right]\right\} \tag{7}$$

$$\begin{aligned} P_i &= \mathrm{Re}\left(V_i Y_{ij}^{*} V_j^{*} - S_i\right) \leq \in \\ Q_i &= \mathrm{Im}\left(V_i Y_{ij}^{*} V_j^{*} - S_i\right) \leq \in \end{aligned} \tag{8}$$

The next linearized PF equations are:

$$\begin{aligned} P_{Gf}-P_{df} &= \sum_{j=1}^{n} V_f Y_{fj} V_j \cos\left(\delta_f-\delta_j-\theta_{fj}\right)+P_{injf} \\ Q_{Gf}-Q_{df} &= \sum_{j=1}^{n} V_f Y_{fj} V_j \sin\left(\delta_f-\delta_j-\theta_{fj}\right)+Q_{injf} \end{aligned} \tag{9}$$

In the same way, bus *t* becomes;

$$\begin{aligned} P_{Gt}-P_{dt} &= \sum_{j=1}^{n} V_t Y_{tj} V_j \cos\left(\delta_t-\delta_j-\theta_{tj}\right)+P_{injt} \\ Q_{Gt}-Q_{dt} &= \sum_{j=1}^{n} V_t Y_{tj} V_j \sin\left(\delta_t-\delta_j-\theta_{tj}\right)+Q_{injt} \end{aligned} \tag{10}$$

where n is the buses number. P_{injf}, Q_{injf}, P_{injt}, and Q_{injt} ($\forall i$) are the FACTS give a jab P and Q at node-*f* and -*t* and the standards of them primarily hinge on the types of FACTS controller.

The initial phase in outcome the optimum result is to figure a LF; $L_{fm}(\boldsymbol{z})$ matching the PF incongruity calculation at buses *f* and *m*, they are obviously modeled in the OPF NM as ECs as:

$$L_{fm}(z) = \lambda_{Pf}\left(P_f + P_{df} - P_{Gf}\right) + \lambda_{Qf}\left(Q_f + Q_{df} - Q_{Gf}\right) \\ +\lambda_{Pm}(P_m + P_{dm} - P_{Gm}) + \lambda_{Qm}(Q_m + Q_{dm} - Q_{Gm}) \tag{11}$$

$$[W]\begin{bmatrix}\Delta x\\ \Delta s\\ \Delta\lambda\end{bmatrix} = -\begin{bmatrix}\nabla_x L\\ \nabla_s L\\ \nabla_\lambda L\end{bmatrix} \Rightarrow [W][\Delta z] = -[\nabla L] \tag{12}$$

where, P_f, P_m, Q_f, Q_m are P and Q fed at nodes *f* and *m*. $P_{Gf}, P_{Gm}, Q_{Gf}, Q_{Gm}$ are P and Q generations at nodes *f* and *m*, correspondingly. $P_{df}, P_{dm}, Q_{df}, Q_{dm}$ are P and Q loads at nodes *f* and *m*, correspondingly. $\lambda_{Pf}, \lambda_{Qf}, \lambda_{Pm}, \lambda_{Qm}$ are LF multipliers at nodes *f* and *m*, and $\boldsymbol{z} = [x \quad s \quad \lambda]^T$,where x, s, λ are vectors of state-control, FACTS and LF multipliers variables.

The initial and subsequent order derivative terms of (11) are to be found in vector $\nabla L_{ft}$and matrix,$\boldsymbol{W}_{ft}$ respectively. These terms are then combined with the gradient vector∇L and matrix W of the entire network for a sparsity-oriented solution [41].

2.2.1. For TCSC

Assuming that, TCSC is connected in between nodes *f* and *m* as shown in Fig. 2. After applying KCL and KVL, the overall transfer AM for the TCSC is created. The components of the branch AM are computed for every branch.

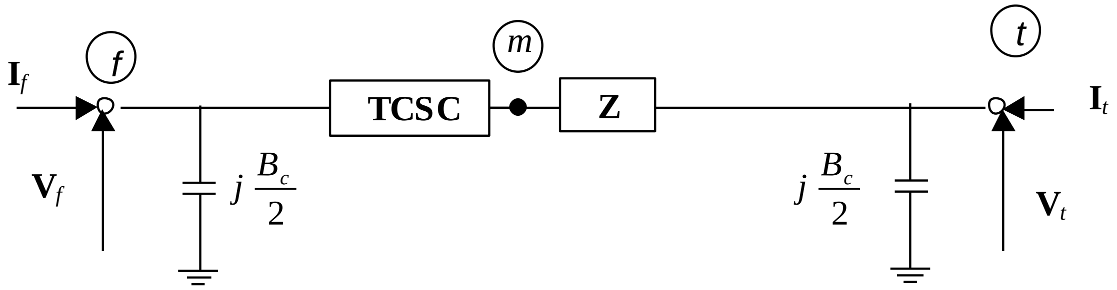

Fig. 2. TS combining TCSC

$$\begin{bmatrix}I_f\\ I_m\end{bmatrix} = \begin{bmatrix}Y_{ff} & Y_{fm}\\ Y_{mf} & Y_{mm}\end{bmatrix}\begin{bmatrix}V_f\\ V_m\end{bmatrix} \tag{13}$$

where,

$$Y_{ff} = Y_{mm} = \frac{1}{X_{TCSC}}, Y_{fm} = Y_{mf} = -\frac{1}{X_{TCSC}} \tag{14}$$

The P_{finj}^{TCSC} and Q_{finj}^{TCSC} injections at bus-*f* can be stated by;

$$P_{finj}^{TCSC} = V_f V_m B_{TCSC} \sin(\delta_f - \delta_m) \\ Q_{finj}^{TCSC} = {V_f}^2 B_{TCSC} + V_f V_m B_{TCSC} \cos(\delta_f - \delta_m) \tag{15}$$

Similarly, the P_{minj}^{TCSC} and Q_{minj}^{TCSC} fed at bus-*m* can be expressed by;

$$P_{minj}^{TCSC} = V_f V_m B_{TCSC} \sin(\delta_m - \delta_f) \\ Q_{minj}^{TCSC} = {V_m}^2 B_{TCSC} + V_f V_m B_{TCSC} \cos(\delta_m - \delta_f) \tag{16}$$

where, $\boldsymbol{B}_{TCSC} = \frac{1}{X_{TCSC}}$and $V_f, V_m, \delta_f, \delta_m$ are the VMs and phase angles at nodes f and m as depicted in Fig. 2.

The LF now includes the PF incompatibility formula at nodes f and m as ECs. The TCSC linked to nodes f and m controls the P flow over branch m-t, as illustrated in Fig. 2. This operational condition is represented in the OPF formulation as an EC that, if the TCSC is configured to regulate a predetermined quantity of P, is active during the iterative process. It should be noted that the LF, $L_{ft}(\boldsymbol{z})$ be made up of $L_{fm}(\boldsymbol{z}) + L_{mt}(\boldsymbol{z})$,

$$L_{mt}(z) = \lambda_{mt}(P_{mt} - P_c) \tag{17}$$

where λ_{mt} is the LF multiplier associated with the P flowing from nodes m to t, and P_c is the desired active PF in the line.

$$\begin{gathered} L_{ft}(\boldsymbol{z}) = \lambda_{Pf}\left(P_f + P_{df} - P_{Gf}\right) + \lambda_{Qf}\left(Q_f + Q_{df} - Q_{Gf}\right) \\ +\lambda_{Pm}(P_m + P_{dm} - P_{Gm}) + \lambda_{Qm}(Q_m + Q_{dm} - Q_{Gm}) + \lambda_{mt}(P_{mt} - P_c) \end{gathered} \tag{18}$$

2.2.2. For UPFC

Employing KCL and KVL to the schematic depicted in Fig. 3 yields an approximate transfer AM for the UPFC. The following equations can be used to calculate the infusion currents for every branch.

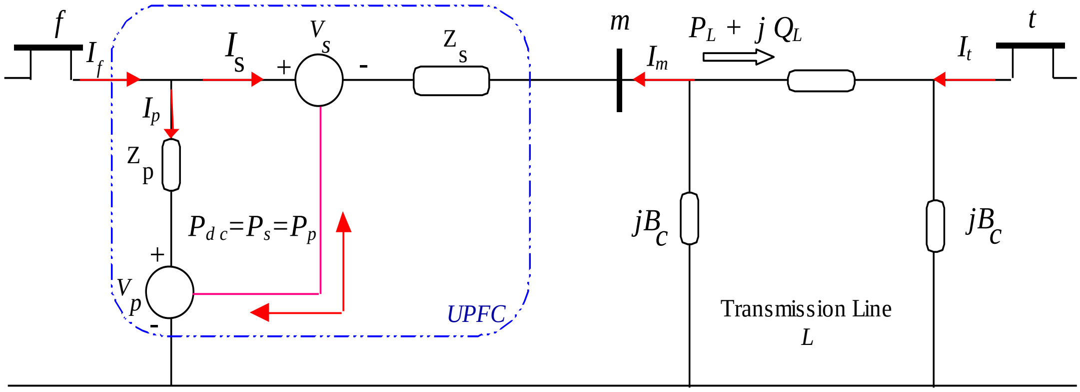

Fig. 3. Connection of investigated UPFC in a TS

$$\begin{bmatrix} I_f \\ I_m \end{bmatrix} = \begin{bmatrix} Y_{ff} & Y_{fm} \\ Y_{mf} & Y_{mm} \end{bmatrix}\begin{bmatrix} V_f \\ V_m \end{bmatrix} + \begin{bmatrix} Y_{fm} & Y_s \\ Y_{mm} & 0 \end{bmatrix}\begin{bmatrix} V_s \\ V_p \end{bmatrix} \tag{19}$$

The P and Q Eqs., are derived: At node f, m in (20) and (21), respectively

$$\begin{aligned} P_f = {} & V_f^{\,2}G_{ff} + V_fV_m\left(G_{fm}\cos(\delta_f - \delta_m) + B_{fm}\sin(\delta_f - \delta_m)\right) \\ & + V_fV_s\left(G_{fm}\cos(\delta_f - \delta_s) + B_{fm}\sin(\delta_f - \delta_s)\right) \\ & + V_fV_p\left(G_p\cos(\delta_f - \delta_p) + B_p\sin(\delta_f - \delta_p)\right) \\ Q_f = {} & -V_f^{\,2}B_{ff} + V_fV_m\left(G_{fm}\sin(\delta_f - \delta_m) - B_{fm}\cos(\delta_f - \delta_m)\right) \\ & + V_fV_s\left(G_{fm}\sin(\delta_f - \delta_s) - B_{fm}\cos(\delta_f - \delta_s)\right) \\ & + V_fV_p\left(G_p\sin(\delta_f - \delta_p) - B_p\cos(\delta_f - \delta_p)\right) \end{aligned} \tag{20}$$

$$\begin{aligned} P_m = {} & V_m^{\,2}G_{mm} + V_fV_m\left(G_{fm}\cos(\delta_m - \delta_f) + B_{fm}\sin(\delta_m - \delta_f)\right) \\ & + V_mV_s(G_{mm}\cos(\delta_m - \delta_s) + B_{mm}\sin(\delta_m - \delta_s)) \\ Q_m = {} & -V_m^{\,2}B_{mm} + V_mV_m\left(G_{fm}\sin(\delta_m - \delta_f) - B_{fm}\cos(\delta_m - \delta_f)\right) \\ & + V_mV_s(G_{mm}\sin(\delta_m - \delta_s) - B_{mm}\cos(\delta_m - \delta_s)) \end{aligned} \tag{21}$$

Furthermore, the P and Q Eqs., for the series and shunt converters are presented in (22), and (23), respectively

$$\begin{aligned}P_s = &\ V_s^2 G_{mm} + V_s V_f\big(G_{fm}\cos(\delta_s-\delta_f) + B_{fm}\sin(\delta_s-\delta_f)\big)\\ &+ V_s V_m(G_{mm}\cos(\delta_s-\delta_m) + B_{mm}\sin(\delta_s-\delta_m))\\ Q_s = &-V_s^2 B_{mm} + V_s V_f\big(G_{fm}\sin(\delta_s-\delta_f) - B_{fm}\cos(\delta_s-\delta_f)\big)\\ &+ V_s V_m(G_{mm}\sin(\delta_s-\delta_m) - B_{mm}\cos(\delta_s-\delta_m))\end{aligned} \tag{22}$$

$$\begin{aligned}P_p &= -V_p^2 G_p + V_p V_f\big(G_p\cos(\delta_p-\delta_f) + B_p\sin(\delta_p-\delta_f)\big)\\ Q_p &= V_p^2 B_p + V_p V_f\big(G_p\sin(\delta_p-\delta_f) - B_p\cos(\delta_s-\delta_f)\big)\end{aligned} \tag{23}$$

Under the assumption of a zero-loss converter, the UPFC does not pump or soak P in relation to the TS. Here, the P required by the series converter (Ps) must be satisfied by the P given to the shunt converter (Pp),

$$P_s + P_p = 0 \tag{24}$$

where Y_{ff} and Y_{mm} are admittance at bus *f*, *m*. Y_{fm} is admittance linking bus *f&t*, Y_s and Y_p are the series and shunt transformer admittances. δ_f and δ_m are the angles of voltage buses *f* and *m* respectively. δ_s and δ_p are the controllable angles of supreme voltage source in lieu of the series and shunt converters respectively. A vital principle in UPFC model [23], is that the P_p necessity gratify the P_s.

$$L_{p-s}(z) = \lambda_{p-s}(P_p + P_s) \tag{25}$$

where λ_{p-s} is the LF multiplier.

The P incinerated at t is expressed as a stream limitation crosswise the outlet that connects f and t. Flow constraints of this type are typically carried out in OPF formulas only in the event that PF limits are surpassed, but in this specific use, this limitation is active during the iterative outcome unless the user elects to disable the limitations. Fig. 3 shows the typical operation scenario as soon as the UPFC is connected.

$$L_{mt}(z) = \lambda_{PL}(P_L - P_c) + \lambda_{QL}(Q_L + Q_c) \tag{26}$$

where λ_{PL} is the LF related with P dose at *t* and λ_{QL} is the LF allied with Q dose at *t*. $P_c$and Q_c are the stated P and Q exit *t*. The UPFC LF that includes each of the previously mentioned separate donations is,

$$L_{UPFC}(z) = L_{fm}(z) + L_{p-s}(z) + L_{mt}(z) \tag{27}$$

i.e.

$$\begin{aligned}L_{UPFC}(\mathbf{z}) = &\ \lambda_{Pf}(P_f + P_{df} - P_{Gf}) + \lambda_{Qf}(Q_f + Q_{df} - Q_{Gf})\\ &+\lambda_{Pm}(P_m + P_{dm} - P_{Gm}) + \lambda_{Qm}(Q_m + Q_{dm} - Q_{Gm})\\ &+\lambda_{p-s}(P_p + P_s) + \lambda_{PL}(P_L - P_c) + \lambda_{QL}(Q_L + Q_c)\end{aligned} \tag{28}$$

In the same way (19) to (28) can be extended for GUPFC.

3. Proposed GA Method

The best location of investigated FACTS tools under a number of limitations is solved using the suggested GA, which has proven to be able to produce precise and workable options in a fair amount of time to compute. Fig. 4 depicts the flowchart of the best location for the FACTS units employing GA, which is also utilized to obtain the OPF options. Ninety-five percent was the crossover rate and one percent was the mutation rate. Several crossover techniques, such as single, double, and uniform, were tested. Nonetheless, this model's bracket crossover produced logical answers. When the suggested approach is used on an IEEE 30-bus system, the best places for TCSCs, UPFCs, and GUPFCs are found. The following part covers the OPF options for minimizing generating costs with FACTS tools positioned in the best lines found by GA.

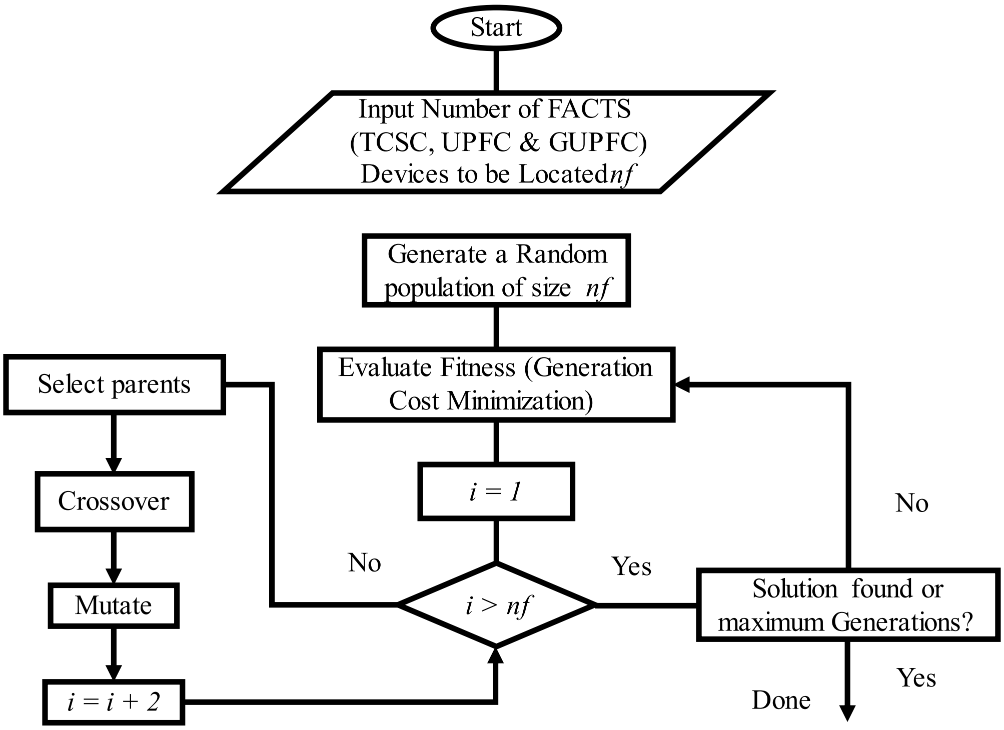

Fig. 4. Identifying the optimum place of FACTS via GA

4. Results and Discussion

The IEEE 30-bus test systems (41 TLs, 4 LTC transformers, and 6 PGs) have been used to demonstrate the efficacy of the suggested technique. The maximum absolute bus power discrepancy convergence margins for all instances here are 1 e^{-8} (0.0001 MW/MVAR). Investigations for the addressed system [46], depicted in Fig. 5, are conducted in order to assess the efficacy of the suggested approach. The goal of OPF ideas is to reduce the generation cost. These solutions have been stretched to multi-type FACTS units after being solved for many scenarios involving multiple TSCSs, UPFCs, and GUPFCs.

4.1. Scenario 1: Multiple TCSCs

Parameters (variable inductance L=0.0150 pu and capacitance C=0.00020 pu) are taken into consideration in order to get OPF ideas with various TCSCs. The study reveals that the TCSC operates in capacitive or inductive modes by default. All TCSC impedances are thought to be permitted to fluctuate between -70% and +20% of the matching outlet impedances. With the desired real PF of the lines (obtained using GA) shown in Table 1, results of the whole GC, TL, TG, Table 2 and Table 3 give the results of the determination of the TCSC reactance and the accompanying firing angles, as well as ACSU that involve one and multi TCSCs.

Table 1. SL–PFs of TCSC

Line (L)#	From bus (B)	To B	Calculated L–PF (MW)	SL–PF (MW)
2	1	3	58.68	65.0
3	2	4	33.88	28.5
6	2	6	45.00	38.5
9	6	7	34.35	30.5

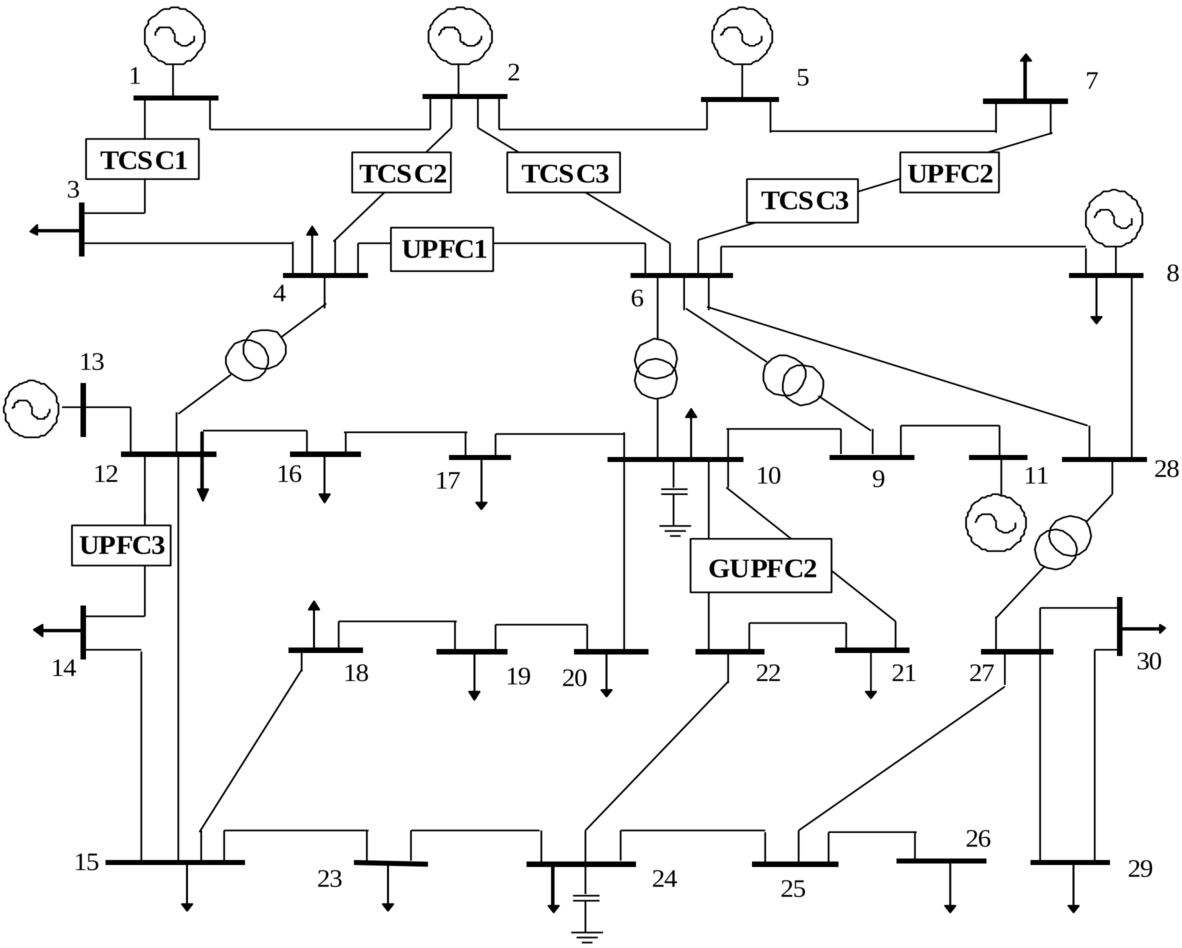

Fig. 5. Investigated system

Table 2. OPF results with 1TCSC

		Lacking TCSC	L 2	L 3	L 6	L 9
V_G(p.u.)	V_1	1.0500	1.0500	1.0500	1.0500	1.0500
	V_2	1.0382	1.0376	1.0380	1.0380	1.0380
	V_5	1.0113	1.0103	1.0116	1.0119	1.0105
	V_8	1.0192	1.0181	1.0196	1.0199	1.0194
	V_{11}	1.0934	1.0930	1.0957	1.0944	1.0934
	V_{13}	1.0886	1.0875	1.0893	1.0896	1.0882
P_G(MW)	P_{G1}	176.14	176.24	176.16	176.20	176.17
	P_{G2}	48.84	48.83	48.84	48.84	48.84
	P_{G5}	21.51	21.52	21.50	21.50	21.50
	P_{G8}	22.15	22.06	22.13	22.10	22.10
	P_{G11}	12.24	12.21	12.23	12.23	12.23
	P_{G13}	12.00	12.00	12.00	12.00	12.00
TAP (%)	T_{11}	4.23	4.298	2.873	3.910	3.910
	T_{12}	-8.481	-8.760	-6.783	-7.888	-7.888
	T_{15}	0.646	0.319	0.826	0.881	0.881
	T_{36}	-5.789	-5.882	-5.751	-5.719	-5.719
α_{final} (degree (D))		-	4.15	15.69	15.22	15.731
X_{TCSC} (pu)		-	-0.038	0.058	0.053	0.0585
$\sum P_G$ (MW)		292.88	292.846	292. 854	292.85	292.842
$\sum P_{loss}$ (MW)		9.478	9.446	9.454	9.442	9.442
$\sum Cost$ ($/hr)		802.404	802.261	802.311	802.262	802.251

Table 3. OPF results with 2 TCSC

Line #.		2&3	2&6	2&9	3&6	3& 9	6& 9
V_G (p.u.)	V_1	1.0500	1.0500	1.0500	1.0500	1.0500	1.0500
	V_2	1.0377	1.0377	1.0374	1.0377	1.0379	1.0380
	V_5	1.0107	1.0110	1.0094	1.0129	1.0108	1.0110
	V_8	1.0186	1.0189	1.0181	1.0214	1.0197	1.0201
	V_{11}	1.0937	1.0950	1.0922	1.0964	1.0965	1.0949
	V_{13}	1.0881	1.0885	1.0867	1.0915	1.0890	1.0891
P_G(MW)	P_{G1}	176.21	176.23	176.05	176.35	176.05	176.05
	P_{G2}	48.84	48.84	48.79	48.88	48.79	48.79
	P_{G5}	21.51	21.50	21.38	21.47	21.40	21.40
	P_{G8}	22.07	22.04	22.27	21.92	22.29	22.28
	P_{G11}	12.21	12.21	12.28	12.16	12.28	12.29
	P_{G13}	12.00	12.00	12.00	12.00	12.00	12.00
TAP (%)	T_{11}	3.944	3.126	4.697	3.568	2.260	3.704
	T_{12}	-8.258	-7.200	-9.220	-7.042	-5.963	-7.573
	T_{15}	0.482	0.575	0.161	1.381	0.765	0.794
	T_{36}	-5.839	-5.811	-5.874	-5.580	-5.731	-5.698
α_{final} (D)	α_2	5.385	5.606	3.529	-	-	-
	α_3	12.920	-	-	19.535	14.242	-
	α_6	-	13.584	-	18.012	-	13.917
	α_9	-	-	16.444	-	14.551	13.700
X_{TCSC2} (pu)		-0.0297	-0.028	-0.0427	-	-	-
X_{TCSC3}(pu)		0.0307	-	-	0.1056	0.0432	-
X_{TCSC6}(pu)		-	0.037	-	0.0850	-	0.0401
X_{TCSC9} (pu)		-	-	0.0663	-	0.0463	0.0380
$\sum P_G$ (MW)		292.84	292.83	292.86	292.777	292.82	292.81
$\sum P_{loss}$ (MW)		9.437	9.426	9.455	9.377	9.417	9.411
$\sum Cost$ ($/hr)		802.234	802.186	802.057	801.967	802.209	802.190

4.2. Scenario 2: Multiple UPFCs

In order to derive OPF remedies with numerous UPFCs, Table 4's variables are taken into account. With the envisioned complex PF for certain of the perfectly chosen lines (gotten using GA) illustrated in Table 5, remedies of the total GC, TL, TG, UPFC control variables (s, p, and V_s), and ACSU in the studied system by including one and multiple UPFCs are identified and provided in Table 6 and Table 7.

Table 4. UPFC variables (pu)

X_s	X_p	V_s^{max}	V_p	S_s^{max}	S_p^{max}
0.02	0.02	0.5	1.0	1.0	1.0

Table 5. S–L–PF of UPFC

Line #	From bus	To bus	PF (S_{ft}) w/o UPFC (MVA)	S S_{ft} (1 UPFC)	S S_{ft} (2 UPFC)
7	6	4	-49.30 + j1.30	-50 + j 2	-
9	6	7	34.35 + j3.63	30 + j 5	26+j2
17	12	14	7.58 + j1.86	8 + j 2	7+j3

4.3. Scenario 3: Multiple GUPFCs

For deriving OPF remedies with numerous GUPFCs, Table 8's variables are taken into account. After including single and multiple GUPFCs, remedies for the total GC, TL, TG, GUPFC settings (δ_{s1}, δ_{s2}, V_{s1}, V_{s2} and δ_p), and ACSU of the studied system are presented in Table 9, with the effectively chosen lines (obtained using GA) displaying the desired complex PF in Table 10.

Table 6. OPF results through 1 UPFC

		No UPFC	L 7	L 9	L 17
V_G(p.u.)	V_1	1.0500	1.0450	1.0098	1.0500
	V_2	1.0382	1.0247	0.988	1.0382
	V_5	1.0113	1.0071	0.9835	1.0115
	V_8	1.0192	1.0111	0.9904	1.0196
	V_{11}	1.0934	1.0290	1.1000	1.1000
	V_{13}	1.0886	1.1000	1. 0983	1.0067
P_G(MW)	P_{G1}	176.14	154.72	163.10	175.29
	P_{G2}	48.84	46.14	44.10	48.59
	P_{G5}	21.51	22.25	15.00	21.42
	P_{G8}	22.15	35.00	30.17	21.37
	P_{G11}	12.24	15.08	14.76	11.76
	P_{G13}	12.00	12.00	13.17	12.00
TAP (%)	T_{11}	4.23	0.474	3.958	2.887
	T_{12}	-8.481	10.00	-10	1.947
	T_{15}	0.646	-7.612	-1.895	4.925
	T_{36}	-5.789	0.205	-7.842	-3.280
δ_s(D)		-	0	156.58	145.1
δ_p(D)			-6.16	-7.83	-11.01
V_s(pu)		-	0.1064	0.1370	0.1093
$\sum P_G$ (MW)		292.88	285.193	280.30	290.435
$\sum P_{loss}$ (MW)		9.478	1.793	12.448	7.035
$\sum Cost$ (\$/hr)		802.404	784.901	765.433	793.869

Table 7. OPF results by 2 UPFC

#.		9 & 17
VG (p.u.)	V1	1. 0044
	V2	0. 9840
	V5	0. 9820
	V8	0. 9899
	V11	1.1000
	V13	1. 0178
PG(MW)	PG1	161. 15
	PG2	43.60
	PG5	15.00
	PG8	29. 11
	PG11	14.18
	PG13	13.28
TAP (%)	T11	0. 215
	T12	2.190
	T15	2.464
	T36	-5. 368
δs(D)		150.31 141.09
δp(D)		-7.74 -10.8
Vs(pu)		0.1445 0. 1078
$\sum P_G$ (MW)		276.325
$\sum P_{loss}$ (MW)		14. 355
$\sum Cost$ (\$/hr)		751.822

Table 8. GUPFC variables (pu)

X_{s1}	X_{s2}	X_p	V_{s1}^{max}	V_{s2}^{max}	V_p	S_{s1}^{max}	S_{s2}^{max}	S_p^{max}
0.02	0.02	0.02	0.5	0.5	1.0	1.0	1.0	1.0

Table 9. S–L–PF

	Line #	Fm bus	To bus	PF (S_{ft}) no GUPFC (MVA)	S S_{ft} (1 GUPFC)	S S_{ft} (2 GUPFC)
GUPFC1	7	6	4	-49.30 + j1.30	-50 + j 2	-50 + j 2
	9		7	34.35 + j3.63	22+j3	22+j3
GUPFC2	27	10	21	15.77 + j 9.24	15+j5	15+j5
	28		22	7.60 + j 4.10	7 + j4	7 + j4

Table 10. OPF results with 1&2 GUPFC

		GUPFC1	GUPFC2	GUPFC1& GUPFC2
P_G(MW)	P_{G1}	142.79	173.39	132.68
	P_{G2}	43.20	48.16	39.32
	P_{G5}	15.00	21.30	15
	P_{G8}	35.00	20.22	35
	P_{G11}	23.45	13.56	25.98
	P_{G13}	12.00	12.00	12.00
TAP (%)	T_{11}	5.426	9.470	-4.327
	T_{12}	10.00	-9.528	10
	T_{15}	-9.99	7.535	-10
	T_{36}	-4.261	1.606	1.284
δ_{s1}(D)		83.93	153	113.44, 147.62
δ_{s2}(D)		148.53	150	137.56, 146
δ_p(D)		-6.16	-11.8	-3.9, -7.9
V_{s1}(pu)		0.0506	0.0712	0.0936, 0.1691
V_{s2}(pu)		0.1425	0.080	0.0744, 0.0834
$\sum P_G$ (MW)		271.438	288.63	259.977
$\sum P_{loss}$ (MW)		13.470	12.124	7.035
$\sum Cost$ ($/hr)		747.011	788.064	714.672

4.4. Scenario 4: Multi-Type (MT) FACTS

For calculating OPF models with MT FACTS, the similar variables indicated directly above will be utilized. Combining MT FACTS with the complex PF in efficiently chosen lines (attained using GA) displayed in Table 11 has allowed for the determination and presentation of approaches to the total GC, TL, TG, control variables (α, δ_{s1}, δ_{s2}, V_{s1}, V_{s2} and δ_p), and ACSU of the investigated system in Table 12 and Table 13.

Table 11. S–L–PF of MT–FACTS

	L #	From B	To B	PF lacking FACTS	S–PF through FACTS
TCSC	6	6	2	45 MW	53 MW
UPFC	9	6	7	(34.35 + j 3.63) MVA	(30 j 5) MVA

Table 12. OPF results with 1 TCSC, UPFC

FACTS		TCSC UPFC
L #		6 9
V_G (pu)	V_1	1.0327
	V_2	1.0112
	V_5	0.9928
	V_8	0.9895
	V_{11}	1.0938
	V_{13}	1. 055
P_G(MW)	P_{G1}	165.20
	P_{G2}	44.90
	P_{G5}	15.00
	P_{G8}	28.00
	P_{G11}	14.03
	P_{G13}	12.64

FACTS		**TCSC**	**UPFC**
L #		**6**	**9**
TAP (%)	T_{11}	-2.847	
	T_{12}	-4.826	
	T_{15}	-3.157	
	T_{36}	-8.043	
α		46.16	-
X_{TCSC}		-0.0970	-
δ_s(D)		-	151.6
δ_p(D)		-	-6.38
V_s(pu)		-	0.1315
$\sum P_G$ (MW)		279.769	
$\sum P_{loss}$ (MW)		12.754	
$\sum Cost$ ($/hr)		762.121	

Table 13. OPF results with 1 TCSC & 1 GUPFC

FACTS		**TCSC**	**GUPFC**
L #		**6**	**7 &9 (Bus-9)**
V_G (pu)	V_1	1.0110	
	V_2	1.0056	
	V_5	0.9905	
	V_8	0.9869	
	V_{11}	1.0119	
	V_{13}	0. 9737	
P_G(MW)	P_{G1}	148.16	
	P_{G2}	43.84	
	P_{G5}	15.00	
	P_{G8}	35.00	
	P_{G11}	17.09	
	P_{G13}	12.00	
TAP (%)	T_{11}	2.438	
	T_{12}	10.00	
	T_{15}	-9.99	
	T_{36}	-4.202	
α		45.41	-
X_{TCSC}		-0.1075	-
δ_s(D)		-	97.71& 145.37
δ_p(D)		-	-4.44
V_s(pu)		-	0.070& 0.1421
$\sum P_G$ (MW)		271.097	
$\sum P_{loss}$ (MW)		13.566	
$\sum Cost$ ($/hr)		740.217	

5. Conclusions

The goal of investigated FACTS is to improve power systems' sustainability, stability, efficiency, and controllability. This study presents an OPF model that uses NM to minimize the GC with multiple and MT-FACTS tools. Applying GA, the best places and sizes for numerous and MT-FACTS tools have been gritty in order to reduce the GC The suggested methods worked well and reached convergence with the fewest number of iterations. The performance of the suggested approaches over a broad range of PF control in the TS has been demonstrated using IEEE 30 bus systems. Additionally, it has been noted that the suggested method is effective and appropriate for improved power management range.

Author Contribution: All authors contributed equally to the main contributor to this paper. All authors read and approved the final paper

Funding: This work has no external funding.

Conflicts of Interest: The authors declare that they have no conflicts of interest.

Data Availability: The data used to support the findings of this study are available at reasonable request from the corresponding author.

Future research directions:

The following points can be studied as a continue of this research:

- The suggested FACTS tools will be used in future studies to develop and expand power systems with thermal and renewable generating units while taking load uncertainties into account.
- The use of modern optimization techniques like the Kepler method is crucial in situations when renewable energy sources introduce more unpredictability and uncertainty into the power system, making it difficult to identify the optimal solution.

Application of the investigated FACTS with recent optimizers in other IEEE systems.

List of abbreviations

Ess: Electrical systems	GUPFC: Generalized unified power flow controller
OPF: Optimal power flow	FACTS: Flexible AC transmission system
GA: Genetic algorithm	SSSC: Static synchronous series compensator
OFs: Objective functions	EIA: Energy Information Administration
PG: Power generation	STATCOM: Static synchronous compensator
LP: Linear programming	TCPST: Thyristor-controlled phase shifting transformer
NM: Newton method	UPFC: Unified power flow controller
TSs: Transmission systems	SVC: Static var compensator
VM: Voltage magnitude	TCSC: Thyristor-controlled series capacitor
EP: Evolutionary programming	TCVR: Thyristor-controlled voltage regulator
EC: Equality constraints	IC: Inequality constraints
VS: Vector space	AM: Admittance matrix
GC: Generation cost	ACSU: Additional control settings of the unit
TL: Transmission losses	TG: Total generation
SL: Specified line	PF: Power flow

References

[1] K. Nusair, F. Alasali, A. Hayajneh, and W. Holderbaum, “Optimal placement of FACTS devices and power-flow solutions for a power network system integrated with stochastic renewable energy resources using new metaheuristic optimization techniques,” *International Journal of Energy Research*, vol. 45, no. 13, pp. 18786–18809, 2021, https://doi.org/10.1002/er.6997.

[2] M. Metwally Mahmoud, “Improved current control loops in wind side converter with the support of wild horse optimizer for enhancing the dynamic performance of PMSG-based wind generation system,” *International Journal of Modelling and Simulation*, vol. 43, no. 6, pp. 952–966, 2023, https://doi.org/10.1080/02286203.2022.2139128.

[3] A. M. Ewias *et al.*, “Advanced load frequency control of microgrid using a bat algorithm supported by a

balloon effect identifier in the presence of photovoltaic power source," *PLoS One*, vol. 18, no. 10, p. e0293246, 2023, https://doi.org/10.1371/journal.pone.0293246.

[4] N. Benalia *et al*., "Enhancing electric vehicle charging performance through series-series topology resonance-coupled wireless power transfer," *PLoS One*, vol. 19, no. 3, p. e0300550, 2024, https://doi.org/10.1371/journal.pone.0300550.

[5] N. F. Ibrahim *et al*., "A new adaptive MPPT technique using an improved INC algorithm supported by fuzzy self-tuning controller for a grid-linked photovoltaic system," *PLoS One*, vol. 18, no. 11, p. e0293613, 2023, https://doi.org/10.1371/journal.pone.0293613.

[6] C. E. Root, "The future beckons [electric power industry]," *IEEE Power and Energy Magazine*, vol. 4, no. 1, pp. 24-31, 2006, https://doi.org/10.1109/MPAE.2006.1578528.

[7] O. M. Kamel, A. A. Z. Diab, M. M. Mahmoud, A. S. Al-Sumaiti, and H. M. Sultan, "Performance Enhancement of an Islanded Microgrid with the Support of Electrical Vehicle and STATCOM Systems," *Energies*, vol. 16, no. 4, p. 1577, 2023, https://doi.org/10.3390/en16041577.

[8] H. Abdelfattah *et al*., "Optimal controller design for reactor core power stabilization in a pressurized water reactor: Applications of gold rush algorithm," *PLoS One*, vol. 19, no. 1, p. e0296987, 2024, https://doi.org/10.1371/journal.pone.0296987.

[9] B. S. Atia *et al*., "Applications of Kepler Algorithm-Based Controller for DC Chopper: Towards Stabilizing Wind Driven PMSGs under Nonstandard Voltages," *Sustainability*, vol. 16, no. 7, p. 2952, 2024, https://doi.org/10.1371/journal.pone.0296987.

[10] U. S. Energy Information Administration, "Annual Energy Outlook 2015 with projections to 2040," *U.S. Department of Energy*, 2015, https://www.nrc.gov/docs/ML1617/ML16172A121.pdf.

[11] R. Kassem *et al*., "A Techno-Economic-Environmental Feasibility Study of Residential Solar Photovoltaic / Biomass Power Generation for Rural Electrification: A Real Case Study," *Sustainability*, vol. 16, no. 5, p. 2036, 2024, https://doi.org/10.3390/su16052036.

[12] M. N. A. Hamid et al., "Adaptive Frequency Control of an Isolated Microgrids Implementing Different Recent Optimization Techniques," *International Journal of Robotics and Control Systems*, vol. 4, no. 3, pp. 1000-1012, 2024, https://doi.org/10.31763/ijrcs.v4i3.1432.

[13] M. M. Mahmoud *et al*., "Voltage Quality Enhancement of Low-Voltage Smart Distribution System Using Robust and Optimized DVR Controllers: Application of the Harris Hawks Algorithm," *International Transactions Electrical Energy Systems*, vol. 2022, no. 1, 2022, https://doi.org/10.1155/2022/4242996.

[14] M. Awad *et al*., "A review of water electrolysis for green hydrogen generation considering PV/wind/hybrid/hydropower/geothermal/tidal and wave/biogas energy systems, economic analysis, and its application," *Alexandria Engineering Journal*, vol. 87, pp. 213-239, 2024, 2023, https://doi.org/10.1016/j.aej.2023.12.032.

[15] N. F. Ibrahim *et al*., "Multiport Converter Utility Interface with a High-Frequency Link for Interfacing Clean Energy Sources (PV\Wind\Fuel Cell) and Battery to the Power System: Application of the HHA Algorithm," *Sustainability*, vol. 15, no. 18, p. 13716, 2023, https://doi.org/10.3390/su151813716.

[16] U. Sultana, A. B. Khairuddin, M. M. Aman, A. S. Mokhtar, and N. Zareen, "A review of optimum DG placement based on minimization of power losses and voltage stability enhancement of distribution system," *Renewable and Sustainable Energy Reviews*, vol. 63. pp. 363-378, 2016, https://doi.org/10.1016/j.rser.2016.05.056.

[17] A. M. Ewais, A. M. Elnoby, T. H. Mohamed, M. M. Mahmoud, Y. Qudaih, and A. M. Hassan, "Adaptive frequency control in smart microgrid using controlled loads supported by real-time implementation," *PLoS One*, vol. 18, no. 4, p. e0283561, 2023, https://doi.org/10.1371/journal.pone.0283561.

[18] I. E. Maysse *et al*., "Nonlinear Observer-Based Controller Design for VSC-Based HVDC Transmission Systems Under Uncertainties," *IEEE Access*, vol. 11, pp. 124014-124030, 2023, https://doi.org/10.1109/ACCESS.2023.3330440.

[19] J. A. Momoh, M. E. El-Hawary and R. Adapa, "A review of selected optimal power flow literature to 1993. II. Newton, linear programming and interior point methods," *IEEE Transactions on Power Systems*, vol. 14, no. 1, pp. 105-111, 1999, https://doi.org/10.1109/59.744495.

[20] M. M. Hussein, T. H. Mohamed, M. M. Mahmoud, M. Aljohania, M. I. Mosaad, and A. M. Hassan, "Regulation of multi-area power system load frequency in presence of V2G scheme," *PLoS One*, vol. 18, no. 9, p. e0291463, 2023, https://doi.org/10.1371/journal.pone.0291463.

[21] M. Chebaani, M. M. Mahmoud, A. F. Tazay, M. I. Mosaad, and N. A. Nouraldin, "Extended Kalman Filter design for sensorless sliding mode predictive control of induction motors without weighting factor: An experimental investigation," *PLoS One*, vol. 18, no. 11, p. e0293278, 2023, https://doi.org/10.1371/journal.pone.0293278.

[22] O. D. Montoya, W. Gil-González, and J. C. Hernández, "Optimal Power Flow Solution for Bipolar DC Networks Using a Recursive Quadratic Approximation," *Energies*, vol. 16, no. 2, p. 589, 2023, https://doi.org/10.3390/en16020589.

[23] R. Divi and H. K. Kesavan, "A Shifted Penalty Function Approach for Optimal Load-Flow," *IEEE Transactions on Power Apparatus and Systems*, vol. PAS-101, no. 9, pp. 3502-3512, 1982, https://doi.org/10.1109/TPAS.1982.317577.

[24] F. G. M. Lima, S. Soares, A. Santos, K. C. Akmeida and F. D. Galiana, "Numerical experiments with an optimal power flow algorithm based on parametric techniques," *IEEE Transactions on Power Systems*, vol. 16, no. 3, pp. 374-379, 2001, https://doi.org/10.1109/59.932271.

[25] J. G. Waight, A. Bose and G. B. Sheble, "Generation Dispatch with Reserve Margin Constraints Using Linear Programming," *IEEE Transactions on Power Apparatus and Systems*, vol. PAS-100, no. 1, pp. 252-258, 1981, https://doi.org/10.1109/TPAS.1981.316836.

[26] G. A. Maria and J. A. Findlay, "A Newton Optimal Power Flow Program for Ontario Hydro EMS," *IEEE Transactions on Power Systems*, vol. 2, no. 3, pp. 576-582, 1987, https://doi.org/10.1109/TPWRS.1987.4335171.

[27] R. C. Burchett and H. H. Happ, "Large Scale Security Dispatching: an Exact Model," *IEEE Transactions on Power Apparatus and Systems*, vol. PAS-102, no. 9, pp. 2995-2999, 1983, https://doi.org/10.1109/TPAS.1983.318104.

[28] S. R. K. Joga *et al*., "Applications of tunable-Q factor wavelet transform and AdaBoost classier for identification of high impedance faults: Towards the reliability of electrical distribution systems," *Energy Exploration & Exploitation*, 2024, https://doi.org/10.1177/01445987241260949.

[29] E. Ghahremani and I. Kamwa, "Maximizing transmission capacity through a minimum set of distributed multi-type FACTS," *2012 IEEE Power and Energy Society General Meeting*, 2012, https://doi.org/10.1109/PESGM.2012.6343906.

[30] M. M. Mahmoud *et al*., "Integration of Wind Systems with SVC and STATCOM during Various Events to Achieve FRT Capability and Voltage Stability: Towards the Reliability of Modern Power Systems," *International Journal of Energy Research*, vol. 2023, no. 1, pp. 1-28, 2023, https://doi.org/10.1155/2023/8738460.

[31] M. M. Mahmoud *et al*., "Application of Whale Optimization Algorithm Based FOPI Controllers for STATCOM and UPQC to Mitigate Harmonics and Voltage Instability in Modern Distribution Power Grids," *Axioms*, vol. 12, no. 5, p. 420, 2023, https://doi.org/10.3390/axioms12050420.

[32] N. F. Ibrahim, A. Alkuhayli, A. Beroual, U. Khaled, and M. M. Mahmoud, "Enhancing the Functionality of a Grid-Connected Photovoltaic System in a Distant Egyptian Region Using an Optimized Dynamic Voltage Restorer: Application of Artificial Rabbits Optimization," *Sensors*, vol. 23, no. 16, p. 7146, 2023, https://doi.org/10.3390/s23167146.

[33] A. Lashkar Ara, A. Kazemi and S. A. Nabavi Niaki, "Multiobjective Optimal Location of FACTS Shunt-Series Controllers for Power System Operation Planning," *IEEE Transactions on Power Delivery*, vol. 27, no. 2, pp. 481-490, 2012, https://doi.org/10.1109/TPWRD.2011.2176559.

[34] A. H. Elmetwaly *et al*., "Modeling, Simulation, and Experimental Validation of a Novel MPPT for Hybrid Renewable Sources Integrated with UPQC: An Application of Jellyfish Search Optimizer," *Sustainability*, vol. 15, no. 6, p. 5029, 2023, https://doi.org/10.3390/su15065209.

[35] M. M. Mahmoud *et al*., "Evaluation and Comparison of Different Methods for Improving Fault Ride-Through Capability in Grid-Tied Permanent Magnet Synchronous Wind Generators," *International*

Transactions on Electrical Energy Systems, vol. 2023, no. 1, pp. 1-22, 2023, https://doi.org/10.1155/2023/7717070.

[36] P. Rajalakshmi and M. Rathinakumar, "An optimal voltage stability enhancement by locating FACTS in optimal place," *Indonesian Journal of Electrical Engineering and Informatics*, vol. 7, no. 1, pp. 105–116, 2019, http://dx.doi.org/10.52549/ijeei.v7i1.810.

[37] M. M. Mahmoud, M. M. Aly, H. S. Salama, and A.-M. M. Abdel-Rahim, "An internal parallel capacitor control strategy for DC-link voltage stabilization of PMSG-based wind turbine under various fault conditions," *Wind Engineering*, vol. 46, no. 3, pp. 983-992, 2022, https://doi.org/10.1177/0309524X211060684.

[38] L. Vanneschi and S. Silva, "Genetic Algorithms," *Lectures on Intelligent Systems*, pp. 45-103, 2023, https://doi.org/10.1007/978-3-031-17922-8_3.

[39] S.-C. Kim and S. R. Salkuti, "Optimal power flow based congestion management using enhanced genetic algorithms," *International Journal of Electrical and Computer Engineering*, vol. 9, no. 2, pp. 875-883, 2019, http://doi.org/10.11591/ijece.v9i2.pp875-883.

[40] T. S. Chung and Y. Z. Li, "Hybrid GA approach for OPF with consideration of FACTS devices*," IEEE Power Engineering Review*, vol. 21, no. 2, pp. 47-50, 2001, https://doi.org/10.1109/MPER.2001.4311272.

[41] S. Panuganti, J. P. Roselyn, S. S. Dash and D. Devaraj, "Contribution of FACTS devices for VSC-OPF problem using Non- Dominated Sorting Genetic Algorithm -II," *2013 International Conference on Energy Efficient Technologies for Sustainability*, pp. 1103-1112, 2013, https://doi.org/10.1109/ICEETS.2013.6533541.

[42] M. Awad, M. M. Mahmoud, Z. M. S. Elbarbary, L. Mohamed Ali, S. N. Fahmy, and A. I. Omar, "Design and analysis of photovoltaic/wind operations at MPPT for hydrogen production using a PEM electrolyzer: Towards innovations in green technology," *PLoS One*, vol. 18, no. 7, p. e0287772, 2023, https://doi.org/10.1371/journal.pone.0287772.

[43] E. ayache Belagra, S. Mouassa, S. Chettih, and F. Jurado, "Optimal power flow calculation in hybrid power system involving solar, wind, and hydropower plant using weighted mean of vectors algorithm," *Wind Engineering*, vol. 48, no. 3, pp. 468-493, 2024, https://doi.org/10.1177/0309524X231212639.

[44] N. P. Padhy and M. A. A. Moamen, "Power flow control and solutions with multiple and multi-type FACTS devices," *Electric Power Systems Research*, vol. 74, no. 3, pp. 341-351, 2005, https://doi.org/10.1016/j.epsr.2004.10.010.

[45] M. E. T. S. Junior and L. C. G. Freitas, "Power Electronics for Modern Sustainable Power Systems: Distributed Generation, Microgrids and Smart Grids—A Review," *Sustainability*, vol. 14, no. 6, p. 3597, 2022, https://doi.org/10.3390/su14063597.

[46] S. A. Mohamed, N. Anwer, and M. M. Mahmoud, "Solving optimal power flow problem for IEEE-30 bus system using a developed particle swarm optimization method: towards fuel cost minimization," *International Journal of Modelling and Simulation*, pp. 1-14, 2023, https://doi.org/10.1080/02286203.2023.2201043.